

Catalysis Science & Technology

Accepted Manuscript



This is an *Accepted Manuscript*, which has been through the Royal Society of Chemistry peer review process and has been accepted for publication.

Accepted Manuscripts are published online shortly after acceptance, before technical editing, formatting and proof reading. Using this free service, authors can make their results available to the community, in citable form, before we publish the edited article. We will replace this *Accepted Manuscript* with the edited and formatted *Advance Article* as soon as it is available.

You can find more information about *Accepted Manuscripts* in the [Information for Authors](#).

Please note that technical editing may introduce minor changes to the text and/or graphics, which may alter content. The journal's standard [Terms & Conditions](#) and the [Ethical guidelines](#) still apply. In no event shall the Royal Society of Chemistry be held responsible for any errors or omissions in this *Accepted Manuscript* or any consequences arising from the use of any information it contains.

Rational design of MoS₂ catalysts: tuning the structure and activity *via* transition metal doping†

Cite this: DOI: 10.1039/x0xx00000x

Charlie Tsai,^{ab} Karen Chan,^{ab} Jens K. Nørskov,^{ab} and Frank Abild-Pedersen^{*b}

Received 00th January 2012,
Accepted 00th January 2012

DOI: 10.1039/x0xx00000x

www.rsc.org/

Density functional theory was used to study how transition metal doping could be used as a method for systematically fine-tuning the structure and activity of MoS₂ catalysts. Through studying the hydrogen evolution reaction (HER) on the edge sites, the role of the metal dopant was determined to be in modifying the strength of sulfur binding on the edge, which determines hydrogen binding onto sulfur atoms on the edge through a negative linear scaling. A simple thermodynamic quantity, ΔG_s , is thus identified, which allows for a description of both the stable structure and adsorption at the edge sites. This provides a descriptor-based framework for the rational design of new MoS₂-type catalysts, where a metal dopant can be chosen to either strengthen or weaken the binding of key intermediates as desired. We also elucidate the unique coverage dependence of hydrogen binding, which explains why MoS₂-type catalysts tend to have near-optimal hydrogen binding. These results are expected to be more general and easily extended to other reactions on other layered transition metal dichalcogenides. Besides confirming the high HER activity of previously studied MoS₂ catalysts, we find 6 additional candidates that show marked improvement in hydrogen adsorption free energies over pristine MoS₂.

Introduction

Two-dimensional layered transition metal dichalcogenides such as MoS₂ have been gaining increased interest as a class of inexpensive electrocatalyst due to their unique chemical and physical properties resulting from their low-dimensionality.¹⁻⁴ Single layered MoS₂ was first predicted by theory⁵ and then shown in a number of experimental studies to be active for the hydrogen evolution reaction (HER) with activity better than most non-precious metals.³⁻¹² The increased activity of nanostructured MoS₂ compared to the inert bulk has been shown to arise from the metallic states located at the edge sites of the monolayer nanoparticles.^{1,6,13-18} Nanostructured MoS₂ has further been suggested¹⁹ and subsequently proven²⁰ as being active for electrochemical CO₂ reduction due to the unique scaling of adsorption energies between key reaction intermediates on the edges.

In light of the wide range of possible applications for MoS₂ catalysts, it is desirable to develop a set of guidelines for rationally designing a new generation of MoS₂-based catalysts, optimized for new sets of reactions. Transition metal doping into the S-edge of MoS₂ has been demonstrated as one method for modifying the edge site activity in both the hydrodesulfurization reaction^{8-10,13,21-23} and HER.^{1,5,9,24} Since the Mo-edge has been predicted to be the active edge for HER,⁵ doping is thought to improve the HER activity by modifying H binding on the S-edge.

Although several detailed theoretical studies^{21,25-28} have already been conducted, they have largely been limited to a few first row transition metal dopants, which is still insufficient for a broad understanding of how transition metals could modify

the structure and activity of MoS₂, particularly in the context of designing new catalysts. A systematic screening of transition metal dopants would provide an explanation of the general effects of doping and what the potentials and limitations are in using doped MoS₂ catalysts for other reactions. Simple descriptors for the trends would also provide underlying intuition for choosing a specific dopant metal.

In this study, we present a density functional theory (DFT) study of 19 transitional metal-doped (Ag, Au, Cu, Co, Cr, Fe, Ir, Mn, Ni, Nb, Os, Pd, Pt, Ta, Re, Rh, Ru, V, W) MoS₂ catalysts. Using HER as a case study, we show that the expected activity can be continuously tuned over a wide range of binding energies through doping. We confirm that previously established MoS₂-type catalysts are active, and propose 6 new candidates that should exhibit improved HER activity over MoS₂ and most pure metal catalysts. Using a simple thermodynamic descriptor, we establish a negative linear scaling relationship between the characteristic binding strength of the edge S on the metal and the adsorption onto the S, which provides a general description of the trends in structure and activity on the edge.

Theoretical approach

We have chosen HER as a model reaction because there is now a rich body of literature for HER on MoS₂-based catalysts. Furthermore, the strength of hydrogen binding on the edge can act as a simple probe for chemical activity since the hydrogen binding is known to scale with that of other key reaction intermediates.²⁹ HER proceeds as $2\text{H}^+ + 2\text{e}^- \rightarrow \text{H}_2$, where hydrogen is bound onto an active site (*) in the first step *via* $\text{H}^+ + \text{e}^- \rightarrow \text{H}^*$. The hydrogen

adsorption free energy was thus determined to be an accurate descriptor of HER activity over transition metal catalysts, with an optimal binding energy of $\Delta G_{\text{H}} = 0$ eV leading to the highest activity.³⁰⁻³² This descriptor-based approach using ΔG_{H} was then extended to transition metal alloys,³³ and used to predict the high activity of edge sites on MoS₂,^{5,6} confirm trends in HER activity on transition metal selenides,³⁴ and predict trends in HER activity on transition metal carbides.³⁵ Due to the largely successful application of the ΔG_{H} descriptor beyond pure transition metals, we also use the hydrogen adsorption free energy, ΔG_{H} , as an indicator of HER activity in this study. A detailed kinetic analysis of the hydrogen evolution reaction is outside the scope of the present work.

Location and concentration of metal dopants

Since we are primarily interested in the trends and developing a general understanding, we focus on the S-edge with 100% of the edge-most Mo atoms substituted by the metal dopant. The reasons for this approximation are: (1) experimentally, Fe, Co, Ni, and Cu doped MoS₂ catalysts have been shown to preferentially substitute at the S-edge with 100% replacement of the Mo atom in many cases;^{1,13,16-18,21-23,36} (2) previous studies on doped MoS₂ clusters^{37,38} have showed that the S-edge is generally less stable and more prone to doping than the Mo-edge, in agreement with detailed scanning tunneling microscopy studies.²³ Hence, even when the Mo-edge is doped, the doped S-edge is expected to also be present. Nevertheless, since partial doping of the S-edge as well as doping of the Mo-edge have been observed,^{21,28} we will return to the implications of these issues within the context of our results later on. We also do not consider the effects of doping into the basal plane in this study.

Determining the stable edge structures

The edge structures of MoS₂ are known to be highly dependent on synthesis and reaction conditions,^{1,21,22,38} making it crucial to consider the relevant conditions in order to accurately describe adsorption and reactivity.³⁹ In this study, we follow a method reported recently for determining the stable edge structures.^{19,34}

An infinite stripe model^{1,5,13,14} was used to investigate the S-edge (shown in Figure 1A). In the infinite stripe, the Mo-edge and the S-edge are both exposed; however, when studying the S-edge, the exact configuration of the Mo-edge is unimportant so long as it is kept constant.

The coverage of H is defined as a fraction of a monolayer with respect to the number of available S atoms on the edge,

$$\theta_{\text{H}} (\text{ML}) = n_{\text{H}} / (\text{S atoms}) \quad (1)$$

and the S coverage is defined as

$$\theta_{\text{S}} (\text{ML}) = n_{\text{S}} / (2 \times \text{edge length}) \quad (2)$$

For each doped S-edge, we considered S coverages of $\theta_{\text{S}} = 0, 0.125, 0.25, 0.5, 0.75,$ and 1.0 ML and H coverages of $\theta_{\text{H}} = 0, 0.25, 0.5, 0.75, 1.0$ ML for each S coverage. Examples of each S and H coverage are shown in Figure 1B. Both metal and S sites were considered at the edge and the H atom was found to

preferentially adsorb onto the edge-most S sites and furthest away from an already adsorbed H, even for the cases where there are S vacancies. In principle, both S and H coverages could vary almost continuously in the ranges considered, but the intermediate coverages to the ones considered here would require large unit cell sizes that are computationally prohibitive.

Using the calculated energies of the infinite stripes with each possible configuration, the free energy of the edge γ was then determined by,

$$\gamma = \frac{1}{2L} \left[G_{\text{stripe}} - \sum_i N_i \mu_i \right] \quad (3)$$

where L is the length of the unit cell, G_{stripe} is the free energy of the infinite stripe, and the sum is over all i constituents of the edge and their respective chemical potentials μ_i and number of atoms N_i . Since we focus on HER in this study, we determined the stable structures under typical HER reaction conditions (i.e., reducing conditions). The chemical potentials at these conditions are determined by the following equilibrium reactions



and



where (*) represents a S vacancy on the edge. Using the computational hydrogen electrode (CHE),^{32,40} the chemical potentials for H and S can be written as

$$\mu(\text{H}) = \frac{1}{2} \mu(\text{H}_2) - eU_{\text{RHE}} \quad (6)$$

$$\mu(\text{S}) = \mu(\text{H}_2\text{S}) - 2 \left(\frac{1}{2} \mu(\text{H}_2) - eU_{\text{RHE}} \right) \quad (7)$$

where U_{RHE} is applied bias defined relative to the reversible hydrogen electrode (RHE) and we have defined the pressure of H₂S to be 10^{-6} bar, corresponding to standard corrosion resistance.^{41,42} This provides all the necessary parameters for determining the free energies of the edges γ .

Since we are interested in the region of low overpotential, we first take the most thermodynamically stable edge configuration at $U_{\text{RHE}} = 0$ V, then we assume that the steady state hydrogen coverage is where H₂ evolution of the final adsorbed hydrogen is more exergonic than either the desorption of HS as H₂S or further H adsorption. This analysis has been used and thoroughly discussed in previous studies as well.^{1,19,22,34} Additional details and a table of the stable structures are included in the ESI†.

In reality, the coverage at $U_{\text{RHE}} < 0$ V would be determined by kinetics, since the pressure of H₂S should be negligible and yet MoS₂ catalysts have been shown to be remarkably stable through potential cycling^{8,43}. However, since activation energies of surface reactions are known to scale with adsorption

energies,^{44,45} we use thermodynamic quantities as an approximation. Our focus is on extracting general guidelines from the trends, so a detailed analysis of the kinetic barriers involved would be outside the scope of this study.

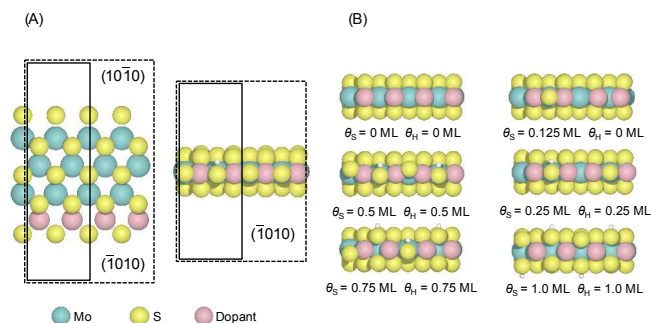


Figure 1. (A) On the left, the top view of the calculation unit cell showing the infinite stripe model with both the Mo-edge and the S-edge exposed. The location of the dopant metal on the S-edge is highlighted in pink. On the right, the front view of the S-edge on the infinite stripe model showing a coverage of $\theta_S = 0.5$ ML and $\theta_H = 0.25$ ML as an example. The dashed lines indicate the unit cells used in this study. The larger unit cell was used to calculate H coverages of $\theta_H = 0.25$ and 0.75 ML, whereas the smaller unit cell was used to calculate coverage of $\theta_H = 0, 0.5$, and 1.0 ML; (B) Examples of each θ_S and θ_H considered for each dopant in this study.

Calculation details

All results were calculated using plane-wave DFT employing ultrasoft-pseudopotentials. The QUANTUM ESPRESSO code⁴⁶ and the BEEF-vdW exchange-correlation functional⁴⁷⁻⁵⁰ were used for all calculations. Recent studies have shown that hydrogen adsorption free energies of MoS₂ calculated using the BEEF-vdW functional agree with those calculated using the RPBE functional previously.^{5,51} The bulk lattice constants for MoS₂ were determined to be $a = 3.19$ Å and $c = 13.05$ Å. Due to the inclusion of van der Waals interactions, both lattice constants are in reasonable agreement with experimental values of $a = 3.16$ Å and $c = 12.29$ Å.^{21,52,53} The plane-wave cutoff and density cutoff were 500 eV and 5000 eV respectively. Further calculation details are summarized in the ESI†.

Results and discussion

Trends in the structure and activity

Doping significantly alters the S and H coverages of the S-edge structure (summarized in Figure 2). There is a general correspondence between the reactivity of the pure transition metal⁵⁴ used for doping and the resulting S coverage at the S-edge (θ_S) (Figure 2A). The noble metal dopants (group 11 metals) have the smallest θ_S , the more reactive metal dopants (group 8 through group 10 metals) have higher θ_S , and the most reactive metal dopants (group 5 through group 7 metals) have the highest θ_S . Within each θ_S , the more reactive dopants generally have smaller θ_H and the more noble dopants have higher θ_H (H coverage increases towards the right of the periodic table). From the edge structures, we observe a general compensation effect between adsorption of S on the metal and the adsorption of H on the S; stronger binding metals have larger S coverages but also smaller H coverages. The effect of transition metal substitution then appears to be in modifying the binding strength of S on the edge (reflected in the S coverage), and in turn,

modifying how strongly the H is bound (reflected in the H coverage).

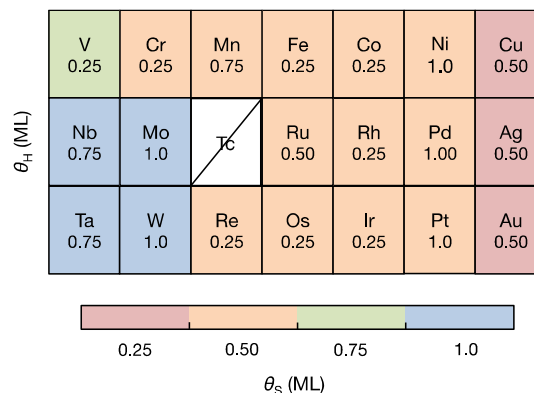


Figure 2. The variation in S coverage (θ_S) and H coverage (θ_H) at the S-edge with choice of dopant metal in the periodic table. The S coverages are indicated by the color and the H coverages are shown in the table. Details of the structural determination and the geometries of the structures are provided in the ESI†.

The H adsorption free energies on the doped edges (ΔG_H) of MoS₂ are almost continuously tuned over a range of approximately -1.0 eV to 0.3 eV (Figure 3). These differential H adsorption free energies were calculated for the final adsorbed H at the stable S and H coverages indicated in Figure 2. For HER, we find 14 doped structures that have ΔG_H closer to thermo-neutral than the S-edge (Pt, Ni, Ru, Rh, Co, Fe, Mn, Ta, V, Nb, Cr, Os, Ir, and Re) and among them, 6 doped structures (Ru, Rh, Co, Fe, Mn, Ta) that have ΔG_H closer to thermo-neutral than the already HER active undoped MoS₂ Mo-edge. Our results confirm the experimentally proven Fe, Ni, and Co-doped MoS₂ S-edges that show improved HER activity over pristine MoS₂,^{9,24} which indicates that our approach of using a single thermodynamic descriptor, ΔG_H , is reasonable.

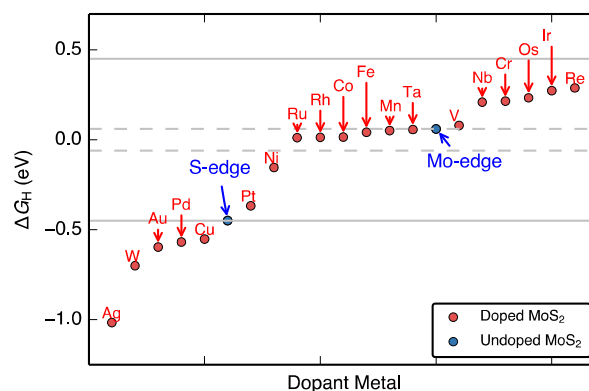


Figure 3. The range of H adsorption free energies (ΔG_H) on each transition metal doped MoS₂. The values of ΔG_H span a range from approximately -1.0 eV to 0.3 eV. The gray lines indicate the range where the doped edges show improved (more thermo-neutral) ΔG_H compared to the pristine MoS₂ S-edge or Mo-edge

Understanding the role of the dopant in modifying adsorption

To understand how the dopant modifies the stability of S on the edge metal relative to the reactivity of the S atom, we employ a thermodynamic descriptor of the characteristic S–metal binding onto the edge. Here we have chosen the adsorption free energy of a single S atom onto the bare metal edge ΔG_S (equivalent to a sulfur

coverage of $\theta_S = 0.125$ ML. Refer to Figure 1A). This is analogous to the bulk cohesive energy per S–metalulfur bond that was proposed by Toulhoat *et al.*,^{25,55,56} and was successfully used as a descriptor for activity on a variety of bulk transition metal sulfides. Our ΔG_S is instead an indicator of the characteristic S–metal bond strength on the edge. We also choose the H adsorption energy onto the single S atom, ΔG_{H-S} , as a descriptor for the characteristic H binding onto the S (hereafter referred to as the characteristic H–S binding). Although the edge structure where ΔG_S is defined is highly unstable under HER conditions, it provides a fixed reference for comparing the variation in S binding on the doped edges. In using only a single S atom, the energetic contribution from structural rearrangements is also minimized, as the rearrangements often result from interactions between neighboring S atoms^{51,57} (see ESI† for all structures and coverages considered herein).

When the S coverages, θ_S , are shown as a function of the metal-S adsorption free energy on the edge, ΔG_S , (Figure 4), the descriptor for metal-S binding on the edge (ΔG_S) is shown to successfully describe the trends in the stable edge structure. The doped edges with the strongest metal-S binding (most negative ΔG_S) have the highest S coverage whereas those with the weakest metal-S binding (most positive ΔG_S) have the lowest S coverage. Generally, nobler metals (such as Ag) have the weakest S binding and more reactive metals (such as W) have the strongest S binding. This is in agreement with previous studies that have found the trend in S–metal bond strength for a doped edge to be Mo > Co > Ni > Cu.^{21,37} In reality, the stable coverages could also be one of the more intermediate S coverages not sampled in this study, and the dependence of θ_S on ΔG_S is expected to be more continuous.

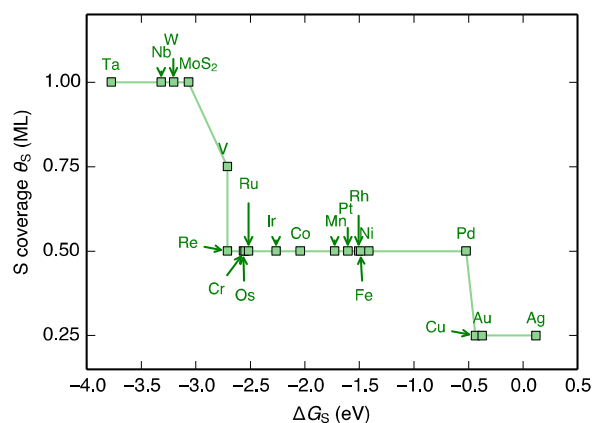


Figure 4. The stable S coverage at the edge θ_S as a function of the metal-S adsorption free energy on the edge ΔG_S .

When the characteristic H–S binding on the edge ΔG_{H-S} is plotted as a function of ΔG_S (Figure 5A), there is a negative linear relationship between the two descriptors, which suggests that there is a compensation effect at play here: stronger S–metal binding should lead to weaker H–S binding. The linear scaling suggests that the characteristic H–S binding energy is entirely determined by how strongly the S–metal binding is, which sets a limit in how the two can be varied with respect to each other. In this way, the dopant

metal plays a central role in mediating the binding of adsorbates onto S.

Plotting the hydrogen adsorption free energy for the stable structures under reaction conditions (ΔG_H) as a function of ΔG_S , we find that the ΔG_S extends beyond the simple compensation effect with ΔG_{H-S} and is also able to describe hydrogen adsorption at the various S and H coverages. Since ΔG_H is used as a descriptor for the HER activity of the catalyst, the HER activity would then be entirely determined by how strongly the dopant metal binds S on the edge. The trends are preserved between Figures 6A and 6B because higher S coverages simply lead to an overall weakening of the S–metal binding, which in turn strengthens the H–S binding. This effect simply decreases the slope of the line in Figure 5A. The success of ΔG_S in describing the trends at the stable coverage suggests that although the correct coverage is crucial in accurately determining the ΔG_H for a given doped edge, the trends are relatively insensitive to the exact coverages. This means that ΔG_S can act as a descriptor for the trends in binding strength on the doped edges regardless of the target reaction conditions. This leads to a general guideline for tuning the reactivity of MoS₂: a stronger binding metal dopant leads to weaker adsorbate binding on the S, and a more noble metal dopant will lead to stronger adsorbate binding on the S.

Note that the existence of S vacancies for some of the doped edges and the possibility of H binding on the metal does not pose a problem for the scaling lines, since hydrogen preferentially binds to the S in those cases. The edges with lower S coverage at the same conditions indicate weaker binding directly to the metal, which corresponds to stronger and preferred binding to the S. This is indeed what our results show (stable structures shown in the ESI†).

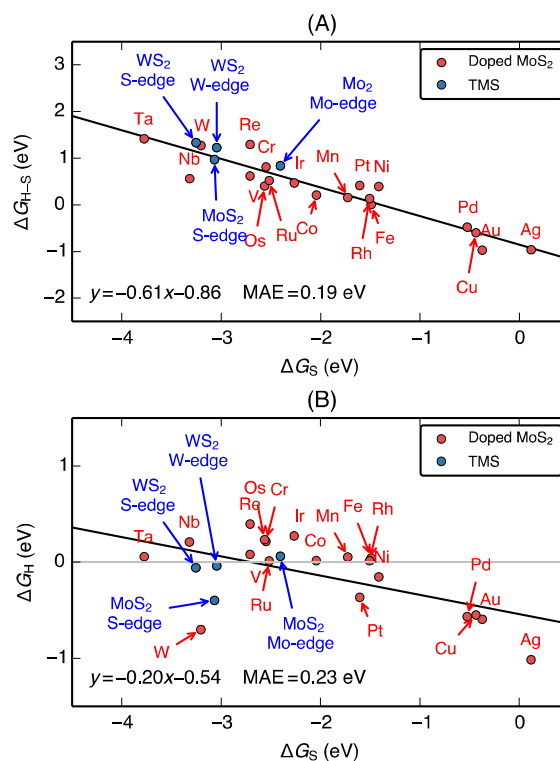


Figure 5. (A) Plot of the characteristic H–S binding energy (ΔG_{H-S}) on the S site as a function of the characteristic S–metal binding energy (ΔG_S) on the metal site.

Weaker S binding to the metal corresponds to stronger H binding to the S. ΔG_S corresponds to a single S adsorbed onto the bare metal edge, whereas ΔG_{H-S} corresponds to a single H bound onto that S (equivalent to $\theta_S = 0.125$ ML and $\theta_H = 0.125$ ML, the lowest possible coverages); (B) Plot of differential H adsorption free energy at the stable coverages for each doped edge (ΔG_H) as a function of the characteristic S-metal adsorption free energy at the edge, ΔG_S (same as in A). ΔG_S acts as a descriptor for the H binding at the various stable coverages. The gray line indicates where $\Delta G_H = 0$ eV. The mean absolute errors (MAE) are ≈ 0.2 eV, which is approximately the error of DFT calculations for adsorption energies. This is reasonable considering that edge reconstruction^{13,34} also contributes greatly to the scatter (additional details in the ESI†).

The ΔG_{H-S} and ΔG_H values for both the pristine S-edge and the pristine M-edge on MoS₂ and WS₂ (values taken from previous studies) scale alongside the doped MoS₂ S-edges, which suggests the negative linear correlation between ΔG_S and ΔG_H is general for transition metal sulfide edges, regardless of the exact local structure. Values of ΔG_S in the range of -4 eV to -2 eV display the most thermo-neutral ΔG_H . Out of all the doped structures, this represents the region where S is bound the most strongly, and hence, where it is the most stable against desorption as H₂S. The optimal doped MoS₂ HER catalysts are thus also expected to be the most stable ones under reaction conditions. Spread in the data results from reconstruction of the S atoms in the edge upon H adsorption, which is especially pronounced for the S-edge of pristine WS₂ and MoS₂, which have a full coverage of S-dimers at the edge at $\theta_S = 1.0$ ML. This phenomena as well as its energetic contributions have been discussed in detail previously.^{51,57} Further information related to edge reconstruction is included in the ESI†.

Although we have focused on the 100% doped S-edge so far, the simple picture formulated by the thermodynamic descriptor ΔG_S could easily be extended to systems where there is partial doping of the S-edge or doping on the Mo-edge. Since both edges appear to follow the same scaling lines for ΔG_S vs. ΔG_H , metal dopants that bind S stronger or weaker than Mo should also shift up or down the scaling line, respectively. Similarly, partial doping of either edge by a transition metal should simply lead to ΔG_S that is intermediate between the pristine MoS₂ edge and that of the 100% transition metal doped edge. Indeed, it has been previously reported that when the concentration of Co dopants is varied, the S-metal binding strength should vary continuously between the pure MoS₂ S-edge and the Co-doped S-edge.²¹

We also note that although the lowest energy configuration of hydrogen was always found to be on a sulfur site, other key reaction intermediates could bind directly to the metal instead, even without the presence of a vacancy. This was shown previously for CO adsorption onto Ni-doped MoS₂ for the electrochemical reduction of CO₂.¹⁹ For such cases ΔG_S would be expected to directly describe the binding strength of the adsorbate, instead of indirectly through the sulfur binding. This then presents an additional compensation effect where the strengthening of one reaction intermediate on the S could lead to the weakening of another reaction intermediate on the metal.

The hydrogen coverage dependence of ΔG_H

The change in the differential H adsorption free energy (ΔG_H) as a function of the H coverage (Figure 6) sheds light on why a large portion of the doped MoS₂ catalysts is predicted to be active HER catalysts. Unlike transition metal surfaces,⁵⁸ the differential energy of H adsorption changes significantly with increasing coverage even before reaching a full monolayer. The reason for this is that for the doped MoS₂ edges, the weakening in H binding results partly from

reorganization of the S atoms at the edge upon H adsorption^{51,57} rather than just adsorbate-adsorbate repulsion (some more information in the ESI). As long as ΔG_H of the first H on the edge is slightly below 0 eV, the ΔG_H at subsequently higher coverages will approach or cross thermo-neutral. This is shown for the pristine Mo-edge, and the Mn, Ni, Nb, and Re doped S-edges in Figure 6. Similar to the transition metals, the coverage effect is more pronounced for surfaces with weaker binding. For doped edges that bind H too strongly (Pd doped MoS₂ for example), ΔG_H will be far from thermo-neutral even at the highest coverage, whereas for doped edges that bind H too weakly (Re doped MoS₂ for example), the higher coverages will only have H binding that is further weakened. The majority of doped edges fall somewhere in between and have some coverage of H where ΔG_H is within 0.2 eV from thermo-neutral.

This presents an important caveat for the design of MoS₂ catalysts for other electrochemical reactions where HER is an unwanted competing reaction. The favourable range of ΔG_H for MoS₂ based catalysts could mean that HER will present issues for selectivity.

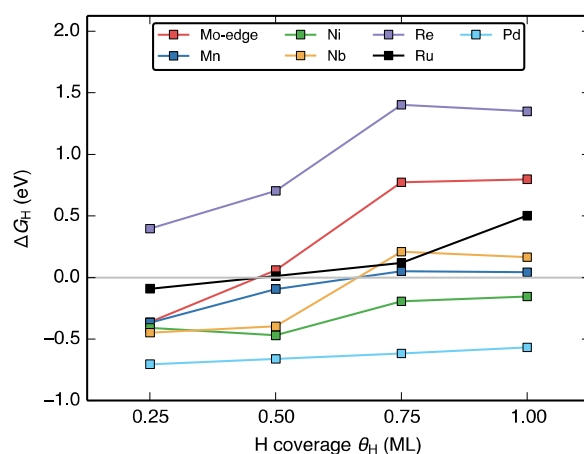


Figure 6. Plot of the variation of the differential H adsorption free energy (ΔG_H) with respect to H coverage (θ_H) of several doped MoS₂ S-edges. The gray line indicates where $\Delta G_H = 0$ eV.

Conclusions

In summary, DFT calculations have been used to investigate the trends in the structure and reactivity of doped MoS₂, where it was found that a wide range of H and S coverages could be achieved. We showed that ΔG_H can almost be continuously tuned to create an optimal catalyst for HER. Through the negatively scaling between ΔG_S (the characteristic metal-S binding at the edge) and ΔG_H , we provide an explanation for the variation: promoting the S-edge with a more reactive metal will lead to weaker H binding, and a less reactive metal will lead to stronger H binding. The success of the ΔG_S descriptor highlights the central role of the edge-most metal in determining structure and activity. Our results provide a simple descriptor-based guideline for the design of MoS₂ catalysts where the dopant metal is chosen to weaken or strengthen key intermediates. We have shown previously that the negative linear scaling between chalcogen (S or Se) binding and H binding on the edge is general for several transition metal dichalcogenides,³⁴ so the concepts developed here could be easily extended for the design of these other catalysts. Furthermore, since the adsorption of H has

been shown to scale with the adsorption of other key reaction intermediates, our results can also be extended to other reactions.

Detailed calculations involving the reaction barriers would be necessary to further validate the trends in HER activity. Future efforts will focus on elucidating the specific reaction mechanism for HER (either Volmer-Tafel or Volmer-Heyrovsky) on layered transition metal sulfides in general. This will be necessary in confirming our approach in screening the activity of these catalysts using the free energy of hydrogen adsorption ΔG_{H} .

The scaling of ΔG_{H} and ΔG_{S} on doped MoS_2 along with other layered transition metal sulfides also suggests that the compensation effect between the binding on the metal and on the S could be a general feature for these materials. The linear scaling relations suggest that certain features of the electronic structure could be exploited in order to further understand the reactivity of transition metal sulfides. Since ΔG_{H} is determined through ΔG_{S} , it is plausible that the d-states of the edge-most transition metal simultaneously determine the S coverage (through the S binding strength on the edge) as well as the adsorption properties onto S sites. However, the binding energies at the edge are often coupled to geometric rearrangements of the edge S atoms upon H adsorption^{1,51,57} and the various S and H coverages, which add an additional layer of complexity to the search. These ideas will be explored in future work.

Acknowledgements

We acknowledge support from the Center on Nanostructuring for Efficient Energy Conversion (CNEEC) at Stanford University, an Energy Frontier Research Center funded by the U.S. Department of Energy, Office of Basic Energy Sciences under award number DE-SC0001060. F.A-P. and J.K.N acknowledge financial support from the U.S. Department of Energy (DOE), Office of Basic Energy Sciences to the SUNCAT Center for Interface Science and Catalysis. C.T. acknowledges support from the National Science Foundation Graduate Research Fellowship Program (GRFP) Grant DGE-114747. K.C. acknowledges support from the Air Force Office of Scientific Research through the MURI program under AFOSR Award No. FA9550-10-1-0572.

Notes and references

^a Department of Chemical Engineering, Stanford University, Stanford, California, 94305, USA

^b SUNCAT Center for Interface Science and Catalysis, SLAC National Accelerator Laboratory, 2575 Sand Hill Road, Menlo Park, California, 94025, USA. E-mail: abild@slac.stanford.edu

† Electronic Supplementary Information (ESI) available: detailed discussion of the methods used to determine the stable edge structure; the structures of all edge configurations considered in this study. See DOI: 10.1039/b000000x/

- M. V. Bollinger, K. W. Jacobsen, and J. K. Nørskov, *Phys. Rev. B*, 2003, **67**, 085410.
- M. Chhowalla, H. S. Shin, G. Eda, L.-J. Li, K. P. Loh, and H. Zhang, *Nat. Chem.*, 2013, **5**, 263–275.
- H. Wang, H. Feng, and J. Li, *Small*, 2014.
- J. Yang and H. S. Shin, *J. Mater. Chem. A*, 2014.
- B. Hinnemann, P. G. Moses, J. L. Bonde, K. P. Jørgensen, J. H. Nielsen, S. Horch, I. Chorkendorff, and J. K. Nørskov, *J. Am. Chem. Soc.*, 2005, **127**, 5308–5309.
- T. F. Jaramillo, K. P. Jørgensen, J. L. Bonde, J. H. Nielsen, S. Horch, and I. Chorkendorff, *Science*, 2007, **317**, 100–102.
- Y. Li, H. Wang, L. Xie, Y. Liang, G. Hong, and H. Dai, *J. Am. Chem. Soc.*, 2011, **133**, 7296–7299.
- J. Kibsgaard, Z. Chen, B. N. Reinecke, and T. F. Jaramillo, *Nat. Mater.*, 2012, **11**, 963–969.
- J. L. Bonde, P. G. Moses, T. F. Jaramillo, J. K. Nørskov, and I. Chorkendorff, *Faraday Discuss.*, 2008, **140**, 219.
- A. B. Laursen, S. Kegnæs, S. Dahl, and I. Chorkendorff, *Energy Environ. Sci.*, 2012, **5**, 5577–5591.
- Z. Chen, A. J. Forman, and T. F. Jaramillo, *J. Phys. Chem. C*, 2013, **117**, 9713–9722.
- H. I. Karunadasa, E. Montalvo, Y. Sun, M. Majda, J. R. Long, and C. J. Chang, *Science*, 2012, **335**, 698–702.
- L. S. Byskov, J. K. Nørskov, B. S. Clausen, and H. Topsøe, *J. Catal.*, 1999, **187**, 109–122.
- M. V. Bollinger, J. V. Lauritsen, K. W. Jacobsen, J. K. Nørskov, S. Helveg, and F. Besenbacher, *Phys. Rev. Lett.*, 2001, **87**, 196803.
- J. Kibsgaard, J. V. Lauritsen, E. Lægsgaard, B. S. Clausen, H. Topsøe, and F. Besenbacher, *J. Am. Chem. Soc.*, 2006, **128**, 13950–13958.
- S. Helveg, J. Lauritsen, E. Lægsgaard, I. Stensgaard, J. K. Nørskov, B. S. Clausen, H. Topsøe, and F. Besenbacher, *Phys. Rev. Lett.*, 2000, **84**, 951–954.
- L. S. Byskov, J. K. Nørskov, B. S. Clausen, and H. Topsøe, *Catal. Lett.*, 2000, **64**, 95–99.
- J. V. Lauritsen, M. V. Bollinger, E. Lægsgaard, K. W. Jacobsen, J. K. Nørskov, B. S. Clausen, H. Topsøe, and F. Besenbacher, *J. Catal.*, 2004, **221**, 510–522.
- K. Chan, C. Tsai, H. A. Hansen, and J. K. Nørskov, *ChemCatChem*, 2014, **6**, 1899–1905.
- M. Asadi, B. Kumar, A. Behranginia, B. A. Rosen, A. Baskin, N. Reppin, D. Pisasale, P. Phillips, W. Zhu, R. Haasch, R. F. Klie, P. Král, J. Abiade, and A. Salehi-Khojin, *Nat. Commun.*, 2014, **5**.
- P. Raybaud, J. Hafner, G. Kresse, S. Kasztelan, and H. Toulhoat, *J. Catal.*, 2000, **190**, 128–143.
- P. G. Moses, B. Hinnemann, H. Topsøe, and J. K. Nørskov, *J. Catal.*, 2009, **268**, 201–208.
- J. Kibsgaard, A. Tuxen, K. G. Knudsen, M. Brorson, H. Topsøe, E. Lægsgaard, J. V. Lauritsen, and F. Besenbacher, *J. Catal.*, 2010, **272**, 195–203.
- D. Merki, H. Vrubel, L. Rovelli, S. Fierro, and X. Hu, *Chem. Sci.*, 2012, **3**, 2515–2525.
- H. Toulhoat, P. Raybaud, S. Kasztelan, G. Kresse, and J. Hafner, *Catal. Today*, 1999, **50**, 629–636.
- A. Travert, H. Nakamura, R. A. van Santen, S. Cristol, J.-F. Paul, and E. Payen, *J. Am. Chem. Soc.*, 2002, **124**, 7084–7095.
- M. Sun, A. E. Nelson, and J. Adjaye, *Catal. Today*, 2005, **105**, 36–43.
- E. Krebs, B. Silvi, and P. Raybaud, *Catal. Today*, 2008, **130**, 160–169.
- C. Shi, H. A. Hansen, A. C. Lausche, and J. K. Nørskov, *Phys. Chem. Chem. Phys.*, 2014, **16**, 4720–4727.
- S. Trasatti, *J. Electroanal. Chem.*, 1971, **33**, 351–378.
- R. Parsons, *Trans. Faraday Soc.*, 1958, **54**, 1053–1063.
- J. K. Nørskov, T. Bligaard, Á. Logadóttir, J. R. Kitchin, J. G. Chen, S. Pandalov, and U. Stimming, *J. Electrochem. Soc.*, 2005, **152**, J23–J26.
- J. Greeley and M. Mavrikakis, *Nat. Mater.*, 2004, **3**, 810–815.
- C. Tsai, K. Chan, F. Abild-Pedersen, and J. K. Nørskov, *Phys. Chem. Chem. Phys.*, 2014, **16**, 13156–13164.
- R. Michalsky, Y.-J. Zhang, and A. A. Peterson, *ACS Catal.*, 2014, 1274–1278.
- J. V. Lauritsen, J. Kibsgaard, G. H. Olesen, P. G. Moses, B. Hinnemann, S. Helveg, J. K. Nørskov, B. S. Clausen, H. Topsøe, E. Lægsgaard, and F. Besenbacher, *J. Catal.*, 2007, **249**, 220–233.
- H. Schweiger, P. Raybaud, and H. Toulhoat, *J. Catal.*, 2002, **212**, 33–38.
- H. Schweiger, P. Raybaud, G. Kresse, and H. Toulhoat, *J. Catal.*, 2002, **207**, 76–87.

39. S. Cristol, J. F. Paul, E. Payen, D. Bougeard, S. Clemendot, and F. Hutschka, *J. Phys. Chem. B*, 2002, **106**, 5659–5667.
40. A. A. Peterson, F. Abild-Pedersen, F. Studt, J. Rossmeisl, and J. K. Nørskov, *Energy Environ. Sci.*, 2010, **3**, 1311.
41. M. Pourbaix, *Atlas D'équilibres Electrochimiques*, Gauthier-Villars, Paris, 1963.
42. H. A. Hansen, J. Rossmeisl, and J. K. Nørskov, *Phys. Chem. Chem. Phys.*, 2008, **10**, 3722–3730.
43. Z. Chen, D. Cummins, B. N. Reinecke, E. Clark, M. K. Sunkara, and T. F. Jaramillo, *Nano Lett.*, 2011, **11**, 4168–4175.
44. Á. Logadóttir, T. H. Rod, J. K. Nørskov, B. Hammer, S. Dahl, and C. Jacobsen, *J. Catal.*, 2001, **197**, 229–231.
45. T. Bligaard, J. K. Nørskov, S. Dahl, J. Matthiesen, C. H. Christensen, and J. Sehested, *J. Catal.*, 2004, **224**, 206–217.
46. P. Giannozzi, S. Baroni, N. Bonini, M. Calandra, R. Car, C. Cavazzoni, D. Ceresoli, G. L. Chiarotti, M. Cococcioni, I. Dabo, A. Dal Corso, S. de Gironcoli, S. Fabris, G. Fratesi, R. Gebauer, U. Gerstmann, C. Gougousis, A. Kokalj, M. Lazzeri, L. Martin-Samos, N. Marzari, F. Mauri, R. Mazzarello, S. Paolini, A. Pasquarello, L. Paulatto, C. Sbraccia, S. Scandolo, G. Sclauzero, A. P. Seitsonen, A. Smogunov, P. Umari, and R. M. Wentzcovitch, *J. Phys.: Condens. Matter*, 2009, **21**, 395502.
47. J. Wellendorff, K. T. Lundgaard, A. Møgelhøj, V. Petzold, D. D. Landis, J. K. Nørskov, T. Bligaard, and K. W. Jacobsen, *Phys. Rev. B*, 2012, **85**, 235149.
48. M. Dion, H. Rydberg, E. Schröder, D. C. Langreth, and B. I. Lundqvist, *Phys. Rev. Lett.*, 2004, **92**, 246401.
49. T. Thonhauser, V. R. Cooper, S. Li, A. Puzder, P. Hyldgaard, and D. C. Langreth, *Phys. Rev. B*, 2007, **76**, 125112.
50. G. Román-Pérez and J. M. Soler, *Phys. Rev. Lett.*, 2009, **103**, 096102.
51. C. Tsai, F. Abild-Pedersen, and J. K. Nørskov, *Nano Lett.*, 2014, **14**, 1381–1387.
52. T. Böker, R. Severin, A. Müller, C. Janowitz, R. Manzke, D. Voß, P. Krüger, A. Mazur, and J. Pollmann, *Phys. Rev. B*, 2001, **64**, 235305.
53. F. Jellinek, G. Brauer, and H. Müller, *Nature*, 1960, **185**, 376–377.
54. B. Hammer and J. K. Nørskov, *Surf. Sci.*, 1995, **343**, 211–220.
55. H. Toulhoat and P. Raybaud, *J. Catal.*, 2003, **216**, 63–72.
56. N. Guernalec, C. Geantet, T. Cseri, M. Vrinat, H. Toulhoat, and P. Raybaud, *Dalton Trans.*, 2010, **39**, 8420–8422.
57. L. S. Byskov, M. V. Bollinger, J. K. Nørskov, B. S. Clausen, and H. Topsøe, *J. Mol. Catal. A-Chem.*, 2000, **163**, 117–122.
58. E. Skúlason, V. Tripkovic, M. E. Björketun, S. Gudmundsdóttir, G. S. Karlberg, J. Rossmeisl, T. Bligaard, H. Jónsson, and J. K. Nørskov, *J. Phys. Chem. C*, 2010, **114**, 18182–18197.